Oct 23rd, 12:00 AM

Effect of Strain Rate on Cold-formed Steel Stub Columns

Maher Kassar

Wei-Wen Yu

Missouri University of Science and Technology, wwy4@mst.edu

Tenth International Specialty Conference on Cold-formed Steel Structures
St. Louis, Missouri, U.S.A., October 23-24, 1990

EFFECT OF STRAIN RATE ON COLD-FORMED STEEL STUB COLUMNS

By M. Kassar[1] and W. W. Yu[2], F. ASCE

INTRODUCTION

The effect of impact loading and associated strain rate on structural strengths of steel columns and flexural members has been the subject of investigation, especially during the last three decades. It was found that theoretical analyses agree well with the experimental results when taking the steel strain rate sensitivity into account for beams (Bodner and Symonds 1962; Rawlings 1963; Aspden and Campbell 1966; Forrestal and Wesenberg 1977). Experimental and theoretical studies indicate that steel columns with large slenderness ratios tested under impact loading may sustain compressive loads in excess of the Euler critical buckling values (Meier 1945; Hoff 1965; Roberts 1972; Logue 1971). This is because the column lateral displacement under rapid loading is less than that from static conditions.

In order for the automotive engineer to achieve a more economical design for car components subjected to impact loads, the effect of strain rate may be considered as a factor in the design. During a vehicle collision the strain rates in the zones of localized deformation can be of the order of 10 to 100 in./in./sec. Consequently, the dynamic capacity of steel compression members is much greater than static value (Wierzbicki 1977). In the analysis of car components subjected to impact loads, the dynamic compressive capacity is considered to be a product of a static crushing strength of the column and a strain rate correction factor depending on the initial impact velocity and the sensitivity of the material to strain rate (Wierzbicki 1977; Wierzbicki and Abramowicz 1979; Abramowicz and Jones 1984).

In cold-formed steel design, local buckling is one of the major design features because of the use of large width-to-thickness ratios of compression elements. The effective width approach has been adopted in several specifications to predict the load-carrying capacities of structural members in buildings and other cold-formed steel structures. Because the effective width formulas included in the current AISI (1986) Specification and the Automotive Steel Design Manual (1986) are primarily based on the results of static tests of cold-formed steel members corresponding to a strain rate of approximately 1.7×10^{-6} in./in./sec., a research project has been conducted at the University of Missouri-Rolla (UMR) under the sponsorship of the American Iron and Steel Institute

---

[1]Engineer II, ABB Impell Corporation, Lincolnshire, Illinois, formerly, Grad. Res. Asst., Univ. of Missouri-Rolla, Rolla, MO.

[2]Curators' Prof. of Civ. Engrg., Univ. of Missouri-Rolla, Rolla, MO.

(AISI) to study the validity of the available effective design formulas for the design of structural members subjected to dynamic loads.

This paper presents the results of 37 stub columns having stiffened and unstiffened elements with various width-to-thickness ratios tested under different strain rates. Comparisons between the tested static and dynamic strengths are presented herein. The findings of the effect of strain rate on mechanical properties of the sheet steel used for fabricating stub columns have been discussed by Kassar and Yu (1990).

EXPERIMENTAL INVESTIGATION

Eighteen (18) box-shaped stub columns were tested for the study of stiffened elements, while 19 I-shaped stub columns were tested for unstiffened elements. All specimens used for this phase of study were fabricated from 35XF low alloy sheet steel. The tensile and compressive mechanical properties of this steel under different strain rates are given in Table 1. The strain rates used in the stub column tests varied from 10^{-5} to 0.1 in./in./sec. The ranges of w/t ratios used in this study were from 26.67 to 53.315 for stiffened elements, and from 8.93 to 20.69 for unstiffened elements.

Test Specimens

The thickness of steel sheets used is 0.085 in (2.2 mm). All specimens were cold-formed by a press brake operation with an inside bend radius of 5/32-in. (4.0 mm) at corners. The length of each stub-column specimen is longer than three times the largest dimension of the cross section of the specimen and less than 20 times the least radius of gyration (Galambos 1988). In all tests, corner strain gages were used to determine maximum edge strains and corresponding stresses. The paired strain gages placed at the tip of unstiffened flanges and at the middle of stiffened flanges were used to determine the strains for critical local buckling loads by using the modified strain reversal method (Johnson and Winter 1966).

Box-Shaped Stub Columns

Eighteen (18) stub column specimens were tested in this study under different strain rates. Box-shaped stub columns were fabricated by connecting two identical hat sections through the unstiffened flanges. High strength bolts (1/4-in. (6.4 mm) dia.) with washers were used for the fabrication of the specimens. The spacing of bolts satisfies the requirements of the AISI Specification (1986). Prior to testing, Both ends of the stub-column specimens were milled to ensure that they were flat and parallel.

The cross section of box-shaped stub column is shown in Fig. 1. The webs of all hat sections were designed to be fully effective. Table 2 gives the average cross sectional dimensions of stub-column specimens and the failure loads. The strain rates used in the tests ranged from 0.0001 to 0.1 in./in./sec.

Eight (8) foil strain gages were used to measure strains at midheight of the stub column specimen. The location of strain gages, numbered from 1 to 8, is shown in Fig. 2.

I-Shaped Stub Columns

In this study, 18 I-shaped stub column specimens have been tested for the study of local buckling and post-buckling strength of unstiffened elements of the 35XF steel material using different strain rates. The strain rates used for the tests ranged from 10^{-5} to 0.1 in./in./sec. Figure 3 shows the cross section of an I-shaped stub column. Table 3 gives the average cross-sectional dimensions of stub column specimens and the failure loads. The stub column specimens were fabricated by bonding two identical channels back to back. Surfaces to be contacted were paper sanded and cleaned with methyl alcohol and bonded by a thin layer of PC-7 epoxy. The webs of the channels were held together by C-clamps after glue was placed on the web. Thin wires (0.002 in. (0.05 mm) dia.) were placed between the channel webs to maintain uniform epoxy thickness. C-clamps were removed after 24 hours. Great care was taken when the stub columns were fabricated. Prior to testing, the ends of stub column specimens were milled flat and parallel.

Fourteen (14) foil strain gages were used to measure strains at the midheight of stub column specimens. The locations of strain gages are shown in Fig. 4.

Test Procedure and Test Results

All stub column specimens were tested in a 110 kips (489 kN) 880 Material Test System (MTS) using stroke (actuator displacement) as the control mode of machine operation to maintain a constant actuator speed. The speed of the actuator is equal to the slope of the function generator programmed ramp. The data acquisition system used in this study consists of 64 simultaneously sampling input channels. Two channels were connected to the MTS machine to record loads and actuator displacements as the test runs. Thirty channels were connected to a 2120 Measurements Group Strain Gage Conditioner and Amplifier System to measure the strain gage outputs. The test frequency or sampling rate depends on the total test time with a maximum of 25,000 readings per seconds for each channel. After the data have been acquired, it was downloaded into the computer for analysis. A Data General mini-computer was used to coordinate the electronic equipment and to store and analyze the test data.

Box-Shaped Stub Columns

Following fabrication of the specimen and placement of strain gages, the stub column was placed in the MTS testing machine. At the beginning of the test, a small preload was applied to the specimen and the resulting strains were recorded for all strain gages to see whether the strain distribution was uniform over the cross section of the specimen. If necessary, thin layers of aluminum foil were added to the ends of stub columns in the regions of low strain. This procedure was repeated until

the strain distribution was essentially uniform over the cross section. Figure 5 shows the box-shaped stub column test setup. The actuator speed was obtained from multiplying the selected strain rate by the overall length of the specimen. Because the maximum actuator speed is 2.5 in./sec., a strain rate higher than 0.1 in./in./sec could not be obtained. The strain rates used in the tests ranged from 10^{-4} to 0.1 in./in./sec. and the corresponding test times ranged from 416 to 0.2 sec.

The failure mode of the specimens varied with the width-to-thickness ratio of the compression flange. For stiffened elements with large w/t ratios, local buckling always occurred in the elastic range. Due to the stress redistribution across the cross section of the compression flange, the edge stress of the stiffened element continued to increase until the maximum edge stress was reached and the specimen failed. For stiffened elements with moderate w/t ratios, the compression flange normally buckled in or near the inelastic range. Yield failure occurred in stiffened elements with small w/t ratios, so that very little, if any, waving of the stiffened compression element occurred before failure. It was noted that the specimens with small w/t ratios failed always at either top or bottom end. The specimens with moderate w/t ratios failed either at the end or at the middle or both, while the specimens with large w/t ratios failed most of the time at or near the middle height of the specimen regardless of the strain rate used in the test. Figure 6 shows a typical failure mode of box-shaped stub column specimens with moderate w/t ratios. For the purpose of comparison, each plot of Fig. 7 presents three typical load-displacement curves for the specimens having the same w/t ratio but tested under different strain rates.

I-Shaped Stub Columns

The test setup for stub-column specimens with unstiffened elements is shown in Fig. 8. The strain rates used in the tests ranged from 10^{-5} to 0.1 in./in./sec. and the corresponding test times ranged from 3600 to 0.2 sec.

During the test, no bonding failure was observed prior to the attainment of the maximum load. The failure modes of stub column specimens with unstiffened elements varied with the width-to-thickness ratios of the unstiffened compression flanges. The unstiffened flanges with large w/t ratios showed large out of plane deformations, whereas the unstiffened compression flanges with small w/t ratios showed no noticeable waving until failure. A typical failure mode of stub column specimens with unstiffened compression flanges is shown in Fig. 9. Each plot of Figure 10 presents three typical load-displacement curves for the specimens having the same w/t ratio but tested under different strain rates.

EVALUATION OF EXPERIMENTAL DATA

The results of tests obtained from this study were evaluated by comparing the tested failure loads with the predicted ultimate load-carrying capacities of stub columns based on the current AISI effective width formulas and using a) static yield stresses and b) dynamic yield stresses corresponding to strain rates used in the tests. Also presented are the ratios of dynamic to static ultimate loads for stub columns having same dimensions but tested under different strain rates. The tested compressive yield stress was used for the evaluation of all stub column specimens studied in this investigation.

Box-Shaped Stub Columns

Box-shaped sections were designed and fabricated for stub column tests to study the post-buckling strengths of stiffened elements by using 35XF sheet steel. All stub columns were subjected to uniform compression. Overall column buckling is prevented by the design of stub columns. All webs of the stub columns were designed to be fully effective based on the 1986 AISI Automotive Design Manual. According to the same manual, unstiffened elements in the sections tested were fully effective.

Critical Local Buckling Load

The critical local buckling loads of box-shaped stub columns can be computed by using the following equation:

$$P_{cr} = A_g f_{cr} \qquad (1)$$

where

f_{cr} = critical local buckling stress of stiffened element
A_g = gross cross-sectional area of stub column.

The total cross-sectional areas of stub columns with stiffened elements are given in Table 4. The critical local buckling stress for each specimen, listed in column (1) of Table 4, is the average value of two critical local buckling stresses of stiffened compression flanges of stub columns. No signs of critical local buckling were observed from the load-strain diagrams of box-shaped stub columns with small and medium w/t ratios (1A and 1B sections).

Table 4 compares the computed and tested critical local buckling loads for stub column specimens fabricated from 35XF sheet steels. The tested critical local buckling loads listed in column (3) were determined from load-strain diagrams by using the modified strain reversal method. The buckling coefficient used to calculate the buckling stress of stiffened elements was equal to 4.0. It is noted from column (4) that the ratio of tested to computed critical local buckling loads $(P_{cr})_{test}/(P_{cr})_{comp}$ increases with increasing strain rate for stub columns with relatively large w/t ratios.

Ultimate Load

A stub column specimen is assumed to attain its ultimate load when the maximum edge stress in the stiffened element reaches the yield stress of steel. The ultimate load-carrying capacities of stub columns can be calculated by using the effective width concept as follows:

$$P_u = A_e F_y \qquad (2)$$

where

F_y = static or dynamic yield stress of steel
A_e = effective cross-sectional area of stub column for the maximum edge stress at F_y.

For the calculation of computed ultimate loads, column (3) in Table 5 uses static yield stress, while column (4) of the same table uses static or dynamic yield stress, corresponding to the strain rate used in the test. The tested failure loads of stub-column specimens are listed in column (5) of Table 5. Comparisons of the computed and tested failure loads of stub columns are shown in columns (6) and (7). As expected, for specimens having same w/t ratios, the tested ultimate load increases with strain rate. The tested to computed ultimate load ratios in column (6) are higher than the corresponding values in column (7).

Tables 6 and 7 were prepared to study the effect of strain rate on failure loads of box-shaped stub column specimens. Table 6 lists average failure loads obtained from tests. For the purpose of comparison, Table 7 shows the ratios of average failure loads obtained from the tests conducted at different strain rates. It is noted from Tables 6 and 7 that 1) the failure load increases with strain rate and 2) the ratio of dynamic to static failure loads increases with increasing w/t ratio. The increase in failure loads is larger at higher strain rates as compared to the increase at lower strain rates.

Figure 11 shows graphically the effect of strain rate on the failure loads of box-shaped stub columns specimens.

I-Shaped Stub Columns

I-shaped stub columns were designed and fabricated to study the post-buckling strengths of unstiffened elements under different strain rates by using 35XF steel. All the stub columns were subjected to uniform compression. Overall column buckling was prevented by the design of the stub columns. The thickness of the web in a stub column was twice the thickness of the unstiffened compression flange because the webs of stub columns were glued together.

Critical Local Buckling Load

The critical local buckling load of an I-shaped stub-column specimen with unstiffened compression elements can be calculated by using Eq. (1), except that f_{cr} is the critical local buckling stress of unstiffened flange. Therfore, a value of 0.43 was used as the buckling coefficient. The total cross-sectional areas of I-shaped stub columns are given in Table 8. The computed and tested critical local buckling loads of specimens fabricated from 35XF steel are given in columns (2) and (3) of Table 8, respectively. The tested critical local buckling loads were determined from load-strain diagrams by using the modified strain reversal method. In Table 8, the tested critical local buckling load for each specimen is the average value of four tested critical local buckling loads determined from four paired strain gages placed at the tips of unstiffened flanges. The computed critical local buckling loads were determined from the product of the average critical local buckling stresses and the gross cross-sectional areas. No critical local buckling was observed from the load-strain diagrams of I-shaped stub columns with small and medium w/t ratios. Note that the critical local buckling loads for stub columns with large w/t ratios tested in the present investigation were underestimated by using Eq. (1). As shown in column (3) of Table 8, the tested critical local buckling load increases with the strain rate.

Ultimate Load

The ultimate load carrying capacities (P_u) of the stub-column specimens can be calculated from Eq. (2).

The computed and tested failure loads of stub columns were compared in columns (3) and (4) of Table 9. Column (3) uses static yield stress, while column (4) uses static or dynamic yield stress according to the strain rate used in the test. Equation (1) was used to compute the failure loads listed in both columns using appropriate yield stresses. The tested ultimate loads of stub columns are listed in column (5). Comparisons of the computed and tested failure loads are listed in columns (6) and (7) of this table. As shown in this table, the ultimate load increases with strain rate. Because column (7) takes into account the effect of strain rate on yield stress, the ratios of tested to computed failure loads listed in column (6) are greater than that given in column (7).

Tables 10 and 11 were prepared to study the effect of strain rate on failure loads for I-shaped stub column specimens. Table 10 lists the average failure loads. For the purpose of comparison, Table 11 shows the ratios of dynamic failure loads. Each value listed in this table is the ratio of two average failure loads for specimens having the same dimensions but tested under different strain rates. It is observed from Tables 10 and 11 that 1) the failure load increases with strain rate and 2) the ratio of dynamic to static failure loads increases with increasing w/t ratio. As noted previously, the increase of failure load is larger at higher strain rates.

Similar to the previous figure, Fig. 12 shows the effect of strain rate on the failure loads of the I-shaped stub column specimens graphically.

CONCLUSIONS

The following conclusions are drawn from this study of the effect of strain rate on structural strengths of cold-formed steel stub columns:

1. The critical local buckling strength and ultimate strength for most of the tests increased with increasing strain rates. The ultimate strengths showed larger increases at higher strain rates than at lower strain rates.

2. The effect of strain rate on stub column strength was found to be similar to those observed from the previous study of material properties as affected by different strain rates. However, ratios of dynamic to static ultimate strengths for the stub columns conducted in this study were found to be slightly higher than those for tensile or compressive material yield stresses.

3. The computed ultimate strength based on the AISI Automotive Design Manual, using static or dynamic yield stress, was found to be conservative for all stub column tests. The mean and standard deviation values for the ratios of tested to computed ultimate strengths were improved by using the dynamic yield stresses rather than the static value for all cases studied in this investigation.

4. In addition to the increase of stub column strength due to material strain rate effect, other factors may contribute to this increase. Similar to long column buckling behavior under dynamic loads as observed by other researchers and discussed in the introduction, local buckling of stiffened and unstiffened elements of cold formed steel members having large w/t ratios may not occur before the section reaches yielding in fast tests. This allows the use of full sectional properties rather than the effective ones. Additional tests with larger w/t ratios than those used in this phase of study are needed to confirm this finding.

Additional tests are being conducted at the University of Missouri-Rolla to investigate the effect of strain rate on member strengths using different sheet steels with various width-to-thickness ratios in order to obtain the needed information for determining the validity of the current effective width design formulas and to develop the improved design recommendations for members subjected to dynamic loads.

ACKNOWLEDGMENTS

This investigation was sponsored by the American Iron and Steel Institute. The technical guidance provided by the AISI Task Force on Automotive Structural Design, under the chairmanship of Dr. S. J. Errera, and the AISI staff (Dr. A. L. Johnson), is gratefully acknowledged. Materials used in the experimental study were donated by LTV Steel Company, Inland Steel Company, and National Steel Corporation.

APPENDIX I. REFRENCES

Abramowicz, W. and Jones, N. (1984). "Dynamic Axial Crushing of Square Tubes." Int. J. Impact Engnr., Vol. 2, No. 2.

Aspden, R. J., and Campbell, J. D. (1966). "The Effect of Loading Rate on the Elasto-Plastic Flexure of Steel Beams."Proceedings of Royal Society of London, Vol. A290.

Automotive Steel Design Manual (1986). 1986 Ed., American Iron and Steel Institute, Washington, D.C.

Bodner, S. R. and Symonds, P. S. (1962). "Experimental and Theoretical Investication of the Plastic Deformation of Cantilever Beams Subjected to Impulsive Loading." Journal of Applied Mechanics, Vol. 29.

Forrestal, M. J. and Wesenberg, D. L. (1977). "Elastic Plastic Response of Simply Supported 1018 Steel Beams to Impulse Loads." Journal of Applied Mechanics, Dec.

Galambos, T. V. (ed.) (1988). Guide to Stability Design Criteria for Metal structures, 4th Edition, New York: John Wiley & Sons.

Hoff, N. (1965). "Dynamic Stability of Structures." Proceedings of an International Conference on Dynamic Stability of Structures Northwestern University, Evanston, Illinois, Oct.

Johnson, A. L. and Winter, G. (1966). "The Structural Performance of Austenitic Stainless Steel Members." Report No. 327, Cornell University, Nov.

Kassar, M. and Yu, W. W. (1990). "Effect of Strain Rate on Material Properties of Sheet Steels." (submitted to ASCE for publication)

Logue, J. M. (1971). "Experimental Study of Thin-Walled Columns Subjected to Impact Loading." Master Thesis, Carnegie-Mellon University, April.

Meier, J. H. (1945). "On the Dynamic of Elastic Buckling." J. Aero. Sci., Vol. 12.

Rawlings, B. (1963). "The Dynamic Behavior of Steel in Pure Flexure." Proc. Royal Soc., Series A, Vol. 275.

Roberts, T. M. (1972). "The Response of Steel Struts to Impact Overload." PhD Thesis, University of Sheffield.

Specification for the Design of Cold-Formed Steel Structural Members (1986). 1986 Ed., American Iron and Steel Institute, Washington, D.C.

Wierzbicki, T. (1977). "Dynamic Crushing of Strain Rate Sensitive Box Columns." SAE Second International Conference on Vehicle Structural Mechanics, April.

Wierzbicki, T. and Abramowicz, W. (1979). "Crushing of Thin-Walled Strain-Rate Sensitive Structures." Dynamic and Crushing Analysis

of Plastic Structures, Euromech Colloquium No. 121, August.

APPENDIX II. NOTATION

The following symbols are used in this paper:

A_e = Effective cross-sectional area of stub columns
A_g = Gross cross-sectional area of stub columns
f_{cr} = Critical local buckling stress
F_y = Yield stress
P_{cr} = Critical local buckling load
P_u = Ultimate load

Table 1

Average Mechanical Properties of 35XF Sheet Steel used in the Experimental Study Under Different Strain Rates

Strain Rate in./in./sec.	$(F_y)_c$ (ksi)	$(F_{pr})_c$ (ksi)	$(F_y)_t$ (ksi)	$(F_u)_t$ (ksi)	Elongation (%)
0.0001	29.83	17.79	32.87	49.35	38.90
0.01	31.92	20.03	36.40	51.76	36.80
1.0	36.91	*****	42.37	56.63	40.90

Notes:

1) 1 ksi = 6.895 MPa
2) $(F_y)_c$ and $(F_{pr})_c$ are based on longitudinal compression coupon tests.
3) $(F_y)_t$ and $(F_u)_t$ and Elongation are determined from longitudinal tension coupon tests.
4) Elongation was measured by using a 2-in. (50.8 mm) gage length.

Table 2

Dimensions of Box-Shaped Stub Columns

Fabricated from 35XF Sheet Steel

Specimen	BF (in.)	BW (in.)	BL (in.)	w/t	Gross Area ($in.^2$)	L (in.)	Tested P_u (kips)
1A1A	2.790	1.492	0.916	27.15	1.2060	12.03	46.12
1A1B	2.811	1.482	0.915	27.39	1.2060	12.02	44.89
1A2A	2.771	1.484	0.918	26.92	1.2010	12.03	50.02
1A2B	2.783	1.482	0.916	27.06	1.2060	12.03	49.29
1A3A	2.804	1.470	0.916	27.31	1.2009	12.03	53.54
1A3B	2.812	1.467	0.915	27.40	1.2009	12.03	54.37
1B1A	3.792	1.990	0.922	38.93	1.5477	14.99	49.19
1B1B	3.812	1.985	0.918	39.17	1.5480	13.97	53.54
1B2A	3.786	1.978	0.918	38.86	1.5412	13.84	56.28
1B2B	3.806	1.982	0.919	39.10	1.5463	13.94	57.01
1B3A	3.786	1.992	0.919	38.86	1.5463	13.84	64.78
1B3B	3.794	1.982	0.918	38.96	1.5440	13.94	60.87
1C1A	4.961	2.523	0.919	52.69	1.9266	15.06	56.76
1C1B	4.984	2.513	0.922	52.96	1.9282	15.06	56.52
1C2A	4.920	2.524	0.920	52.20	1.9203	14.81	61.02
1C2B	4.993	2.519	0.922	53.06	1.9317	15.12	64.58
1C3A	5.000	2.526	0.919	53.15	1.9343	15.09	73.96
1C3B	5.021	2.510	0.922	53.39	1.9334	15.00	69.27

Notes:

1) 1 in. = 25.4 mm

2) 1 kip = 4.448 kN

3) 1 in^2= 645.16 mm^2

See Fig. 1 for the cross section of box-shaped stub columns

Table 3

Dimensions of I-Shaped Stub Columns

Fabricated from 35XF Sheet Steel

Specimen	BC (in.)	D (in.)	w/t	Gross Area ($in.^2$)	L (in.)	Tested P_u (kips)
2A1A	1.000	2.000	8.93	0.6220	7.90	25.26
2A1B	1.010	2.018	9.04	0.6285	7.97	25.35
2A2A	1.000	2.040	8.93	0.6288	7.95	26.04
2A2B	1.015	2.002	9.10	0.6275	7.94	27.70
2A3A	1.000	2.040	8.93	0.6288	7.98	31.41
2A3B	1.003	2.014	8.96	0.6254	7.94	29.41
2B1A	1.375	3.025	13.34	0.9238	9.95	34.20
2B1B	1.381	2.981	13.41	0.9184	9.97	34.20
2B2A	1.380	2.987	13.40	0.9190	9.96	36.30
2B2B	1.378	3.007	13.37	0.9217	9.94	37.52
2B3A	1.375	3.020	13.34	0.9229	10.01	41.67
2B3B	1.382	3.006	13.42	0.9229	9.99	42.70
2C0A	2.000	3.000	20.69	1.1320	14.00	36.30
2C1A	2.014	2.976	20.85	1.1327	14.00	37.23
2C1B	2.006	3.018	20.76	1.1371	13.94	37.66
2C2A	2.024	2.967	20.97	1.1346	14.09	41.28
2C2B	2.010	3.015	20.81	1.1380	13.95	41.52
2C3A	2.020	2.970	20.93	1.1337	14.06	47.92
2C3B	2.015	2.977	20.87	1.1332	13.91	46.16

Notes:

1) 1 in. = 25.4 mm

2) 1 kip = 4.448 kN

3) 1 in^2= 645.16 mm^2

See Fig. 3 for the cross section of I-shaped stub columns

Table 4
Comparison of Computed and Tested Critical Local Buckling Loads
Box-Shaped Stub Columns (Based on k=4.0)

Specimen	f_{cr} (ksi) (1)	$(P_{cr})_{comp}$ (kips) (2)	$(P_{cr})_{test}$ (kips) (3)	(3)/(2) (4)
1A1A	28.35	34.19	N/A	N/A
1A1B	28.32	34.15	N/A	N/A
1A2A	30.30	36.39	N/A	N/A
1A2B	30.28	36.52	N/A	N/A
1A3A	32.16	38.62	N/A	N/A
1A3B	32.15	38.61	N/A	N/A
1B1A	26.79	41.46	N/A	N/A
1B1B	26.75	41.41	N/A	N/A
1B2A	28.55	44.00	N/A	N/A
1B2B	28.51	44.08	N/A	N/A
1B3A	30.22	46.73	N/A	N/A
1B3B	30.20	46.63	N/A	N/A
1C1A	24.25	46.72	50.56	1.082
1C1B	24.20	46.66	50.90	1.091
1C2A	25.83	49.60	58.09	1.171
1C2B	25.63	49.51	55.94	1.130
1C3A	26.88	51.99	66.15	1.272
1C3B	26.81	51.83	65.51	1.264
Mean				1.168
Standard Deviation				0.076

Notes: 1 kip = 4.448 kN

N/A indicates that local buckling did not occur prior to the attainment of the computed load, $(P_u)_{comp}$, given in Table 5.

Table 5
Comparison of Computed and Tested Failure Loads Based on the Effective Width Formulas in the 1986 AISI Automotive Steel Design Manual for Box-Shaped Stub Columns

Spec.	Strain Rate (in./in./sec.)	w/t	$(P_u)_{comp}$, kips Based on $(F_y)_s$	$(P_u)_{comp}$, kips Based on $(F_y)_d$	$(P_u)_{test}$ kips	(5)/(3)	(5)/(4)
	(1)	(2)	(3)	(4)	(5)	(6)	(7)
1A1A	0.0001	27.15	35.97	35.97	46.12	1.28	1.28
1A1B	0.0001	27.39	35.97	35.97	44.89	1.25	1.25
1A2A	0.01	26.92	35.82	38.33	50.02	1.40	1.30
1A2B	0.01	27.06	35.82	38.35	49.29	1.38	1.29
1A3A	0.10	27.31	35.82	40.90	53.54	1.49	1.31
1A3B	0.10	27.40	35.82	40.90	54.37	1.52	1.33
1B1A	0.0001	38.93	46.17	46.17	49.19	1.06	1.06
1B1B	0.0001	39.17	46.18	46.18	53.54	1.16	1.16
1B2A	0.01	38.86	45.97	49.20	56.28	1.22	1.14
1B2B	0.01	39.10	46.13	49.31	57.01	1.23	1.16
1B3A	0.10	38.86	46.13	52.36	64.78	1.40	1.24
1B3B	0.10	38.96	46.06	52.25	60.87	1.32	1.16
1C1A	0.0001	52.69	54.10	54.10	56.76	1.05	1.05
1C1B	0.0001	52.96	54.06	54.06	56.52	1.05	1.05
1C2A	0.01	52.20	54.06	57.38	61.02	1.13	1.06
1C2B	0.01	53.06	54.13	57.46	64.58	1.19	1.12
1C3A	0.10	53.15	54.18	60.88	73.96	1.36	1.21
1C3B	0.10	53.39	54.08	60.76	69.27	1.28	1.14
Mean						1.265	1.184
Standard Deviation						0.139	0.093

Note : 1 kip = 4.448 kN

Table 6
Average Tested Failure Loads for Box-Shaped Stub Columns

Strain Rate	Failure Load, $(P_u)_{test}$, kips		
in./in./sec.	w/t		
	26.67	38.44	53.15
0.0001	45.50	51.36	56.64
0.01	49.65	56.64	62.80
0.1	53.95	62.82	71.48

Table 7
Ratios of Average Ultimate Loads for Box-Shaped
Stub Columns Having Stiffened Flanges

w/t	$(P_u)_2/(P_u)_1$	$(P_u)_3/(P_u)_1$
29.67	1.09	1.18
38.44	1.10	1.22
53.15	1.11	1.26

Notes :

$(P_u)_1$= Average ultimate load for stub column specimens tested at strain rate of 0.0001 in./in./sec.

$(P_u)_2$= Average ultimate load for stub column specimens tested at strain rate of 0.01 in./in./sec.

$(P_u)_3$= Average ultimate load for stub column specimens tested at strain rate of 0.1 in./in./sec.

Table 8
Comparison of Computed and Tested Critical Local Buckling Loads
I-Shaped Stub Columns (Based on k=0.43)

Specimen	$(f_{cr})_{comp}$ (ksi) (1)	$(P_{cr})_{comp}$ (kips) (2)	$(P_{cr})_{test}$ (kips) (3)	(3)/(2) (4)
2A1A	28.34	17.63	N/A	N/A
2A1B	28.30	17.79	N/A	N/A
2A2A	30.26	19.03	N/A	N/A
2A2B	30.20	18.95	N/A	N/A
2A3A	32.17	20.23	N/A	N/A
2A3B	32.16	20.11	N/A	N/A
2B1A	26.50	24.48	N/A	N/A
2B1B	26.47	24.31	N/A	N/A
2B2A	28.19	25.91	N/A	N/A
2B2B	28.21	26.00	N/A	N/A
2B3A	29.85	27.55	N/A	N/A
2B3B	29.80	27.50	N/A	N/A
2C0A	21.81	24.69	35.42	1.434
2C1A	21.71	24.59	36.44	1.482
2C1B	21.78	24.77	36.44	1.471
2C2A	22.78	25.85	40.40	1.563
2C2B	22.92	26.08	40.35	1.547
2C3A	23.70	26.87	46.95	1.747
2C3B	23.76	26.92	44.38	1.648
Mean				1.556
Standard Deviation				0.102

Note: 1 kip = 4.448 kN

N/A indicates that local buckling did not occur prior to the attainment of the computed load, $(P_u)_{comp}$, given in Table 9.

Table 9
Comparison of Computed and Tested Failure Loads Based on the Effective Width Formulas in the 1986 AISI Automotive Steel Design Manual for I-Shaped Stub Columns

Spec.	Strain Rate (in./in./sec.)	w/t	$(P_u)_{comp}$, kips Based on $(F_y)_s$	$(P_u)_{comp}$, kips Based on $(F_y)_d$	$(P_u)_{test}$ kips	(5)/(3)	(5)/(4)
	(1)	(2)	(3)	(4)	(5)	(6)	(7)
2A1A	0.0001	8.93	18.55	18.55	25.26	1.36	1.36
2A1B	0.0001	9.04	18.75	18.75	25.35	1.35	1.35
2A2A	0.01	8.93	18.76	20.07	26.04	1.39	1.30
2A2B	0.01	9.10	18.72	20.03	27.70	1.48	1.38
2A3A	0.10	8.93	18.76	21.42	31.41	1.67	1.47
2A3B	0.10	8.96	18.65	21.30	29.41	1.58	1.38
2B1A	0.0001	13.34	27.49	27.49	34.20	1.24	1.24
2B1B	0.0001	13.41	27.30	27.30	34.20	1.25	1.25
2B2A	0.01	13.40	27.32	29.02	36.30	1.33	1.25
2B2B	0.01	13.37	27.42	29.12	37.52	1.37	1.29
2B3A	0.10	13.34	27.47	30.89	41.67	1.52	1.35
2B3B	0.10	13.42	27.43	30.82	42.70	1.56	1.38
2C0A	0.00001	20.69	29.31	29.26	36.30	1.24	1.24
2C1A	0.0001	20.85	29.21	29.21	37.23	1.27	1.27
2C1B	0.0001	20.76	29.41	29.41	37.66	1.28	1.28
2C2A	0.01	20.97	29.19	30.87	41.28	1.41	1.34
2C2B	0.01	20.81	29.40	31.11	41.52	1.41	1.33
2C3A	0.10	20.93	29.19	32.65	47.92	1.64	1.47
2C3B	0.10	20.87	29.22	32.82	46.16	1.58	1.41
Mean						1.417	1.334
Standard Deviation						0.136	0.070

Note : 1 kip = 4.448 kN

Table 10
Average Tested Failure Loads for I-Shaped Stub Column Specimens with Unstiffened Flanges

Strain Rate	Failure Load, $(P_u)_{test}$, kips		
in./in./sec.	w/t		
	8.93	13.34	20.69
0.0001	25.30	34.20	37.44
0.01	26.87	36.91	41.40
0.1	30.41	42.18	47.04

Table 11
Ratios of Ultimate Loads for I-Shaped Stub Column Specimens Having Unstiffened Flanges

w/t	$(P_u)_2/(P_u)_1$	$(P_u)_3/(P_u)_1$
8.93	1.06	1.20
13.34	1.08	1.23
20.69	1.11	1.26

Notes :

$(P_u)_1$= Average ultimate load for I-shaped stub column specimens tested at strain rate of 0.0001 in./in./sec.

$(P_u)_2$= Average ultimate load for I-shaped stub column specimens tested at strain rate of 0.01 in./in./sec.

$(P_u)_3$= Average ultimate load for I-shaped stub column specimens tested at strain rate of 0.1 in./in./sec.

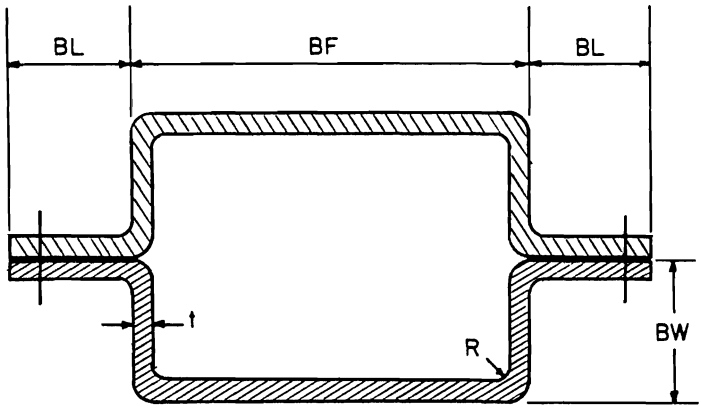

Fig. 1 Cross Sections of Box-Shaped Stub Columns

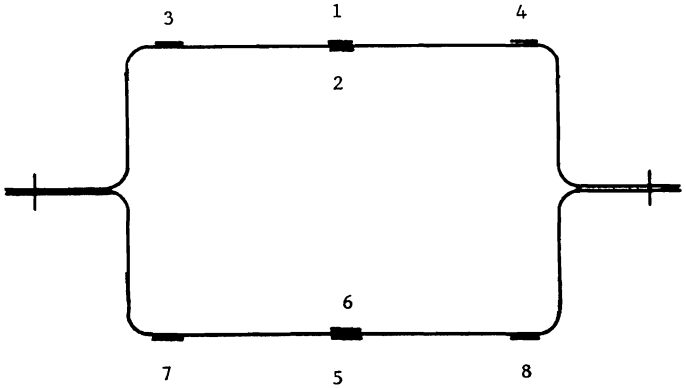

Fig. 2 Locations of Strain Gages at Midheight of Box-Shaped Stub Columns

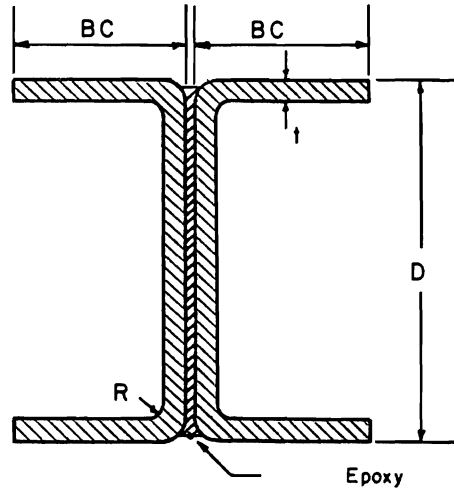

Fig. 3 Cross Sections of I-Shaped Stub Columns

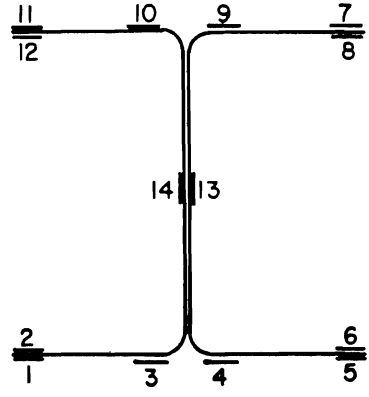

Fig. 4 Locations of Strain Gages at Midheight of I-Shaped Stub Columns

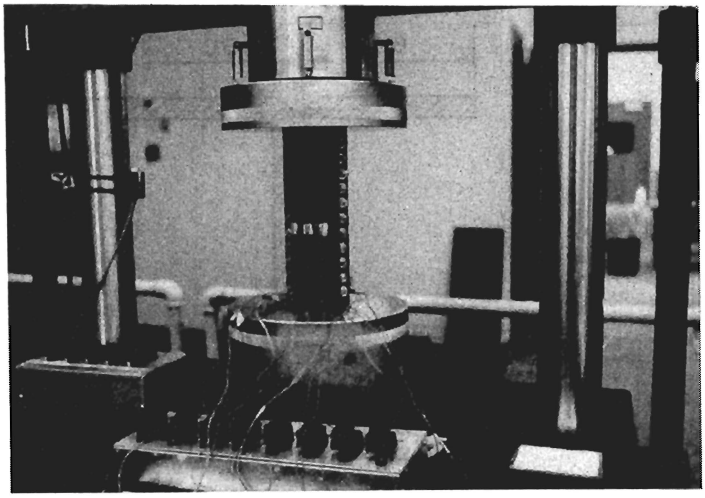

Fig. 5 Test Setup of Box-Shaped Stub Columns

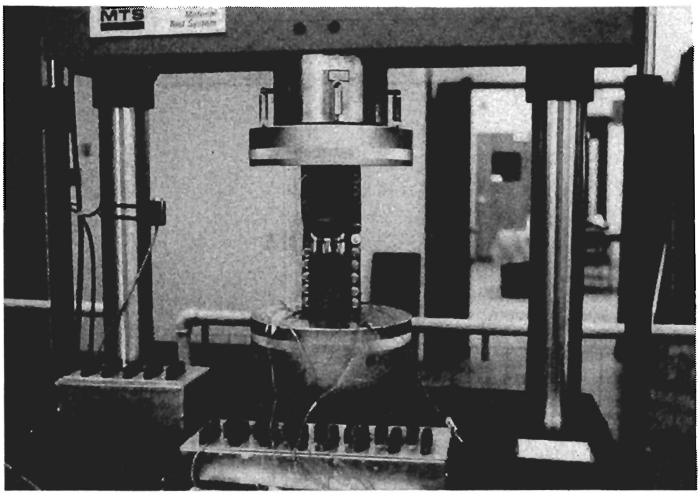

Fig. 6 Failure of Box-Shaped Stub Columns

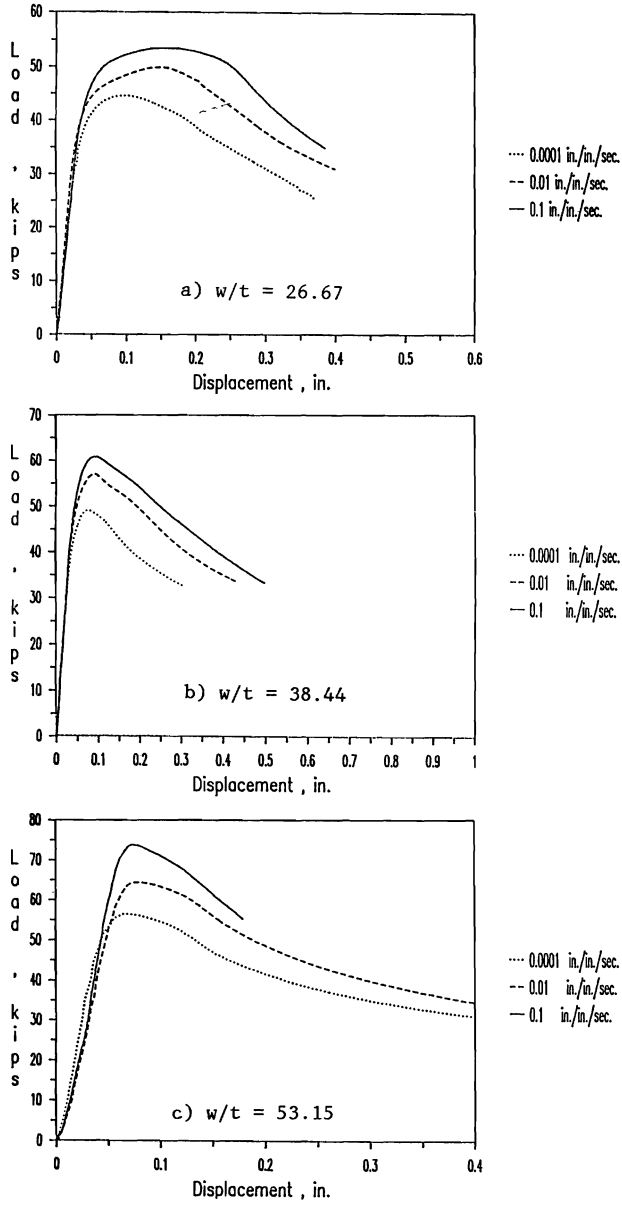

Fig. 7 Load-Displacement Curves for Box-Shaped Stub Columns

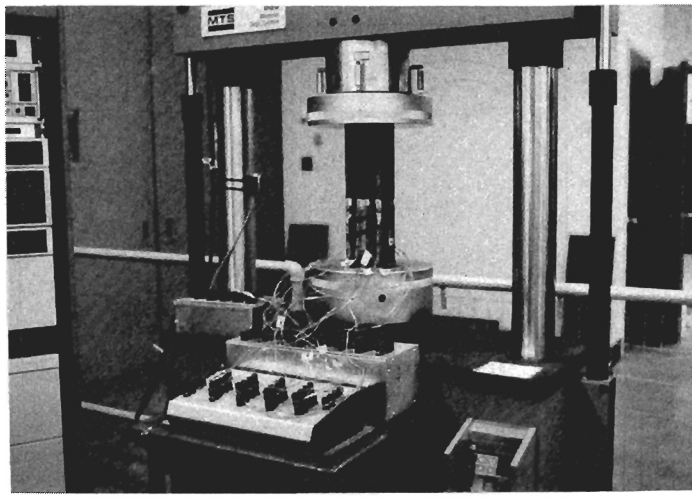

Fig. 8 Test Setup of I-Shaped Stub Columns

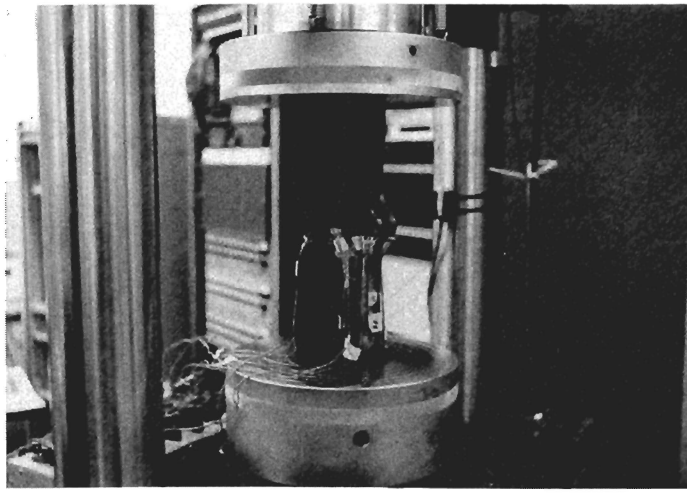

Fig. 9 Failure of I-Shaped Stub Columns

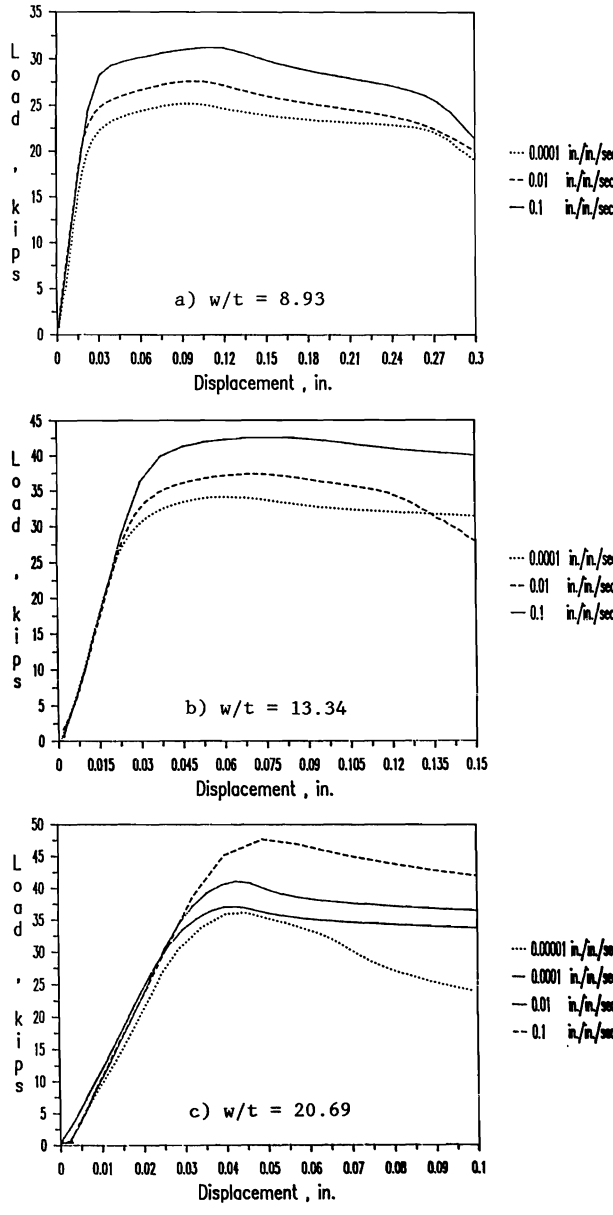

Fig. 10 Load-Displacement Curves for I-Shaped Stub Columns

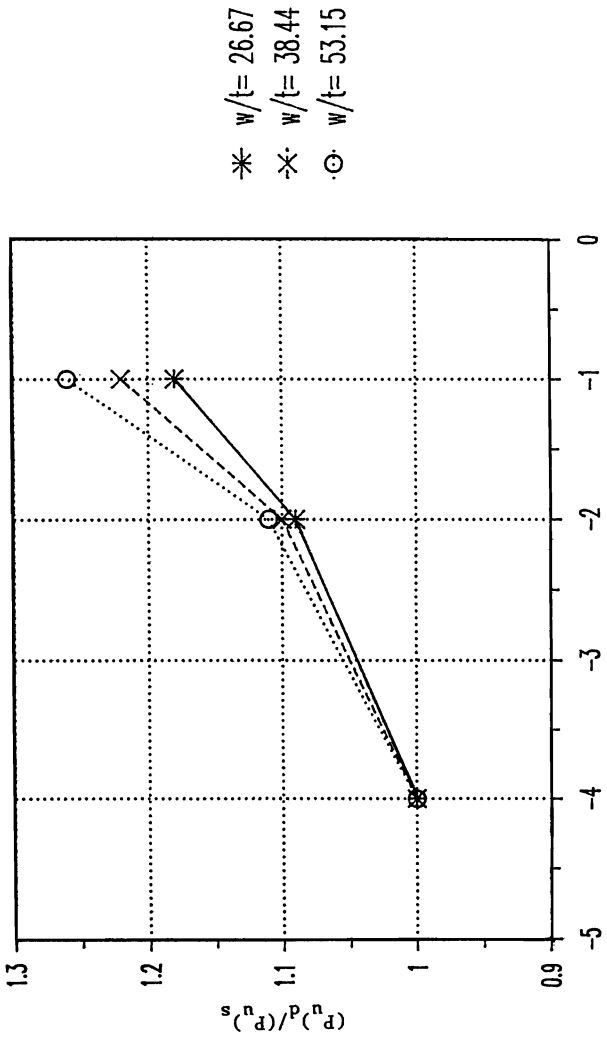

Fig. 11 Ratios of Dynamic to Static Ultimate Loads for Box-Shaped Stub Columns

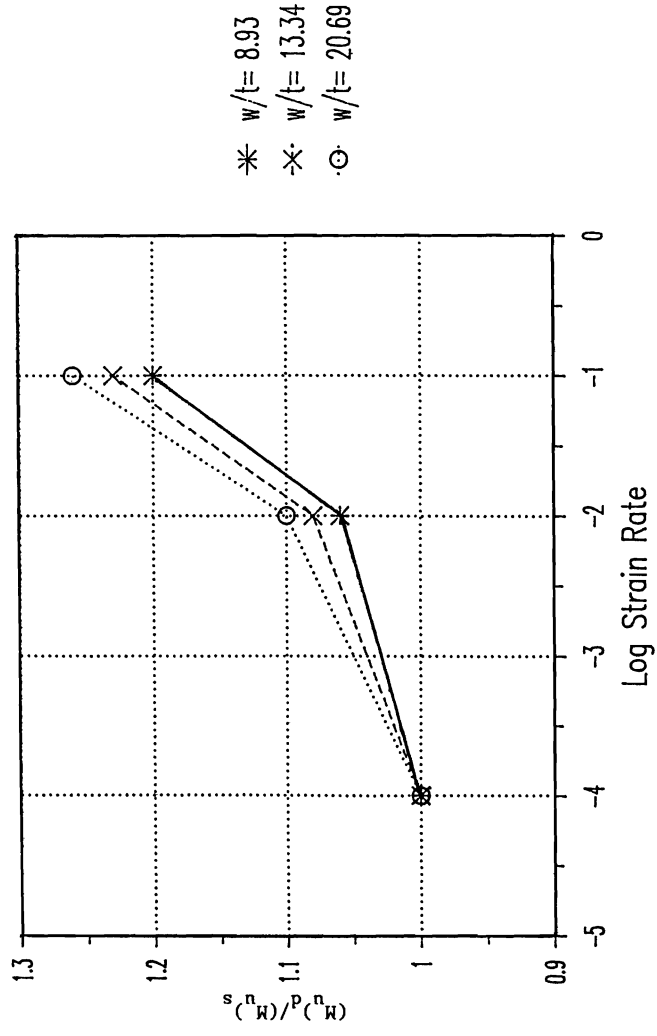

Fig. 12 Ratios of Dynamic to Static Ultimate Loads for I-Shaped Stub Columns